# Catalytic Decomposition of Ammonia over Bimetallic CuO/CeO$_2$ Nanoparticle Catalyst

## Chang-Mao Hung[*]

*Department of Industry Engineering and Management, Yung-Ta Institute of Technology & Commerce,*

*Pingtung 909, Taiwan, Republic of China*

## Abstract

The oxidation of ammonia to nitrogen by selective catalytic oxidation (NH$_3$-SCO) over a bimetallic CuO/CeO$_2$ nanoparticle catalyst at temperatures between 423 and 673K. A bimetallic CuO/CeO$_2$ nanoparticle catalyst was prepared by co-precipitation method at molar ratio of 6:4. This study also considers how the concentration of influent NH$_3$ ($C_0$ = 800 ppm), the space velocity ($GHSV$ = 92000/hr), the relative humidity ($RH$ = 12%) and the concentration of oxygen ($O_2$ = 4%) affect the operational stability and the capacity for removing NH$_3$. The catalysts were characterized before and after reaction using EDX, BET, ATR-FTIR, PSA and TEM. The catalytic performance show that the ammonia was removed by oxidation in the presence of bimetallic CuO/CeO$_2$ nanoparticle catalyst, and around 98% at complete NH$_3$ reduction was achieved, and a high selectivity toward N$_2$ during catalytic oxidation over the catalyst at 673K with an oxygen content of 4.0%. Moreover, the effect of the reaction temperature on the removal of NH$_3$ in the gaseous phase was also monitored at a gas hourly space velocity of under 92000/hr.

*Keywords:* Selective catalytic oxidation (SCO); Tubular fixed-bed reactor (TFBR); Ammonia; Bimetallic CuO/CeO$_2$ nanoparticle catalyst.

## INTRODUCTION

Nowadays, ammonia (NH$_3$) is used in the ammonium nitrate and nitric acid production industry, livestock feedlots, urea manufacturing plants, the nitrogen fertilizer application industry, fossil fuel combustion and petroleum refineries as well as the refrigeration industry (Ng *et al.*, 2007; Chou *et al.*, 2007; Xu *et al.*, 2008). As is known, ammonia is a toxic inorganic gas with a pungent odor under ambient conditions, and is potentially harmful to public health (Geng *et al.*, 2008; Lin *et al.*, 2008). Conventional biological, physical and chemical treatments, including biofilters, stripping, scrubbing with
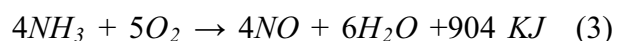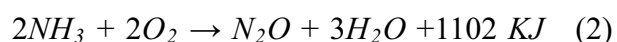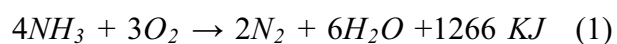
_____

[*]Corresponding author: TEL: +886-8 723-3733 ext 508;

*Fax:* +886-8722-8046

*E- mail address:* hungcm1031@gmail.com

water, post-combustion control, microwave-plasma discharge, electrochemical oxidation and the use of activated carbon fibers for soot adsorption, only trigger a phase transformation and may yield a contaminated sludge and/or an adsorbent, both of which require further treatment. The maintenance and operating costs associated with these physical and/or chemical methods are high. Therefore, the removal and the control and prevention, of the emission of ammonia emission from air and waste streams are important due to environmental concerns.

More recently, catalytic oxidation has been established to increase the effectiveness of advanced oxidation processes technology using dedicated catalysts, which potentially shorten the reaction times of oxidation, and allow it to proceed under milder operating conditions. The selective catalytic oxidation of ammonia ($NH_3$-SCO) in a stream to molecular nitrogen and water is one method for solving problems of ammonia pollution (Dravell *et al.*, 2003). The catalytic oxidation of ammonia has been reported to precede as follows the exothermic global reactions:

$$4NH_3 + 3O_2 \rightarrow 2N_2 + 6H_2O + 1266 \ KJ \quad (1)$$

$$2NH_3 + 2O_2 \rightarrow N_2O + 3H_2O + 1102 \ KJ \quad (2)$$

$$4NH_3 + 5O_2 \rightarrow 4NO + 6H_2O + 904 \ KJ \quad (3)$$

The SCO process that involves ammonia should be selective for nitrogen (reaction 1), and prevent further oxidation of nitrogen (reactions 2 and 3). Earlier work on ammonia oxidation was reviewed by Il'chenko (1976), who focused on the reaction mechanism of ammonia oxidation, and compared catalytic activities. Few catalysts have been used in oxidizing ammonia in the gaseous phase. For instance, Wang *et al.* (1999), who developed Ni-based catalysts for oxidizing fuel gas generated by gasifying biomass, found that fresh Ni-based catalysts were more active at lower temperatures in decomposing ammonia, and the partial pressure of hydrogen in the flue gas is a critical factor that governed ammonia oxidation. Moreover, Liang (2000) studied the oxidation of ammonia in a fixed-bed microreactor in the temperature range 873-1023K at GHSV=1800-3600/hr. They found that the conversion of ammonia reached 98.7% and 99.8% on nitrided $MoNx/\alpha$-$Al_2O_3$ and $NiMoNy/\alpha$-$Al_2O_3$ catalysts, respectively. Schmidt-Szałowski (1998) also developed a hypothetical model of the effect of these catalysts and their activity and selectivity in oxidizing ammonia. Recently, Pansare and Jr. Goodwin (2008) summarized the catalytic oxidation of ammonia in the presence of synthesis gas produced from biomass gasification by tungsten-based catalyst in the temperature range 738-923K. There is a significant effect of the catalyst calcinations temperature, which is the material with the highest ammonia reduction activity.

Copper and cerium metals with fluorite-type oxides have been used to elucidate the reduction characteristics of methane conversion (Kundakovic *et al.*, 1998). The interaction between copper and the cerium is complex, because various Cu-Ce

interactions can result in synergistic effects and oxygen vacancies, enhancing catalytic characteristics (Skårman *et al*., 2002; Hung, 2006). However, little work has been undertaken on the use of Cu-Ce composite metal catalyst to determine the reactive characteristics of these active metals in catalytic oxidation. Due to these properties, the activity of the bimetallic $CuO/CeO_2$ nanoparticle catalyst in the oxidation of ammonia given various values of parameters and its effect on the removal of ammonia in selective catalytic oxidation processes ($NH_3$-SCO) were studied. For these purpose, different techniques approach using EDX, BET, ATR-FTIR, PSA and TEM were employed to examine the behavior of bimetallic $CuO/CeO_2$ nanoparticle catalyst.

## MATERIALS AND METHODS

### Preparing bimetallic $CuO/CeO_2$ nanoparticle catalyst

Bimetallic $CuO/CeO_2$ nanoparticle catalyst used in this work were prepared by the by the co-precipitation of copper (II) nitrate (GR grade, Merck, Darmstadt, Germany) and cerium (III) nitrate (GR grade, Merck, Darmstadt, Germany) at molar ratio of 6:4. The composite catalysts were then calcined at 773K in an airstream for four hours. The resulting powder was made into tablets using acetic acid as a binder. The tablets were later reheated at 573K to burn the binder out of the $CuO/CeO_2$ composite tablets. The tablets were then crushed and sieved into various particle sizes ranging from 0.25-0.15 mm for use later.

### Characterizing the solid phase

The composition of the catalyst's surface was determined using an energy-dispersive x-ray spectrometer (SEM/EDX, JEOL, JSM-6400, Kevex, DeltaII). The amount of carbonaceous deposit on the used bimetallic $CuO/CeO_2$ nanoparticle catalyst surface was determined by carbon-hydrogen-nitrogen elemental analysis (Carlo Erba, model EA 1108, Milan, Italy). The specific surface areas of the composite catalysts were determined by the physical adsorption of nitrogen at 77K using a Brunauer, Emmett, and Teller model and a BET surface area analyzer (ASAP 2000, Micromeritics, Norcross, Georgia). Diffuse reflectance ATR-FTIR spectra of species adsorbed on the catalyst were measured at room temperature using a Bruker Vector 22 FTIR spectrometer, equipped with a diffuse reflectance attachment with a resolution of 4/cm (Bruker, Germany). The changes in the sizes of the catalytic particles were measured using a laser light-scattering particle size analyzer (PSA, Coulter LS100, USA). Transmission electron microscopy (TEM) (Philips CM-200 Twin, Netherlands) elucidated the morphology of the catalysts and yielded information on the distribution of copper-cerium species on the catalyst surface.

### Catalytic tests

Experiments were conducted on a tubular fixed-bed flow quartz reactor (TFBR). Two flowing gases, $NH_3$ and $O_2$, were used to prepare the feed mixture in the diluting gas, helium, which flowed into the inlet of the reactor. A mass flow regulator was used to
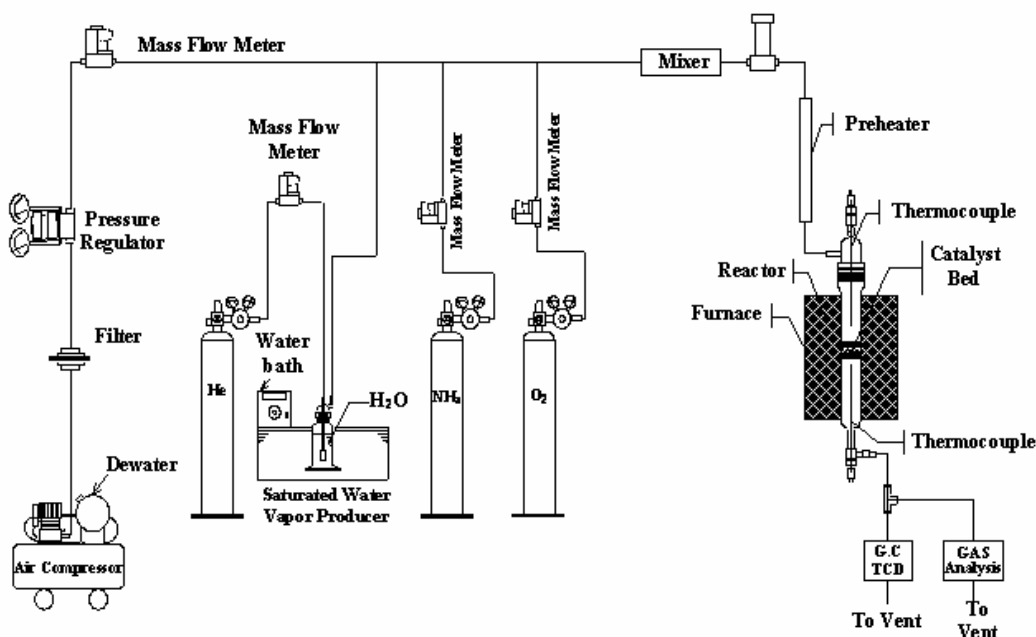
**Fig. 1.** Schematic diagram of the tubular fixed-bed reaction (TFBR) system.

control independently the flows of ammonia and oxygen. Extremely pure helium was used as a carrier gas at a flow rate from 8-13 L/min, controlled using a mass flow meter (830 Series Side-Trak$^{TM}$, Sierra, Monterey, CA, USA). The mass of each catalyst was 1 g and the empty bed volume was approximately 1.2 cm$^3$. An inert material formed from (hydrophilic and inert) $\gamma$-Al$_2$O$_3$ spheres was used to increase the interfacial area between the solid and the gas phase to increase the mass transfer of ammonia from gaseous streams. This approach resembled that of Hung *et al.* (2008), who conducted experiments on the catalytic oxidation of ammonia. A reaction tube with a length of 300 mm and an inner diameter of 28-mm was placed inside a split tube furnace. The tube that contained the catalyst was placed in the same furnace. The temperature was measured using two type-K thermocouples (KT-110, Kirter, Kaohsiung, Taiwan), each with a

diameter of 0.5 mm, these were located in front of and behind the catalytic bed. The thermocouples were also connected to a PID controller (FP21, Shimaaen, Tokyo, Japan) to maintain the temperature in the tube within $\pm$ 0.5%. The concentration of the feed gas (GHSV, 92000 mL/h-g) was maintained at 1000 ppm NH$_3$ and the O$_2$ concentration was 4%. The catalyst was not deactivated during testing. Fig. 1 schematically depicts the tubular fixed-bed reaction system (TFBR).

*Catalytic performance measurement*

Before and after the reaction, samples were automatically injected through a sampling valve into a gas chromatograph (Shimadzu GC-14A), equipped with a thermal conductivity detector. A stainless-steel column (Porapak Q 80/100mesh) was used to separate and determine the concentrations of N$_2$O isothermally at 373K. The areas associated with the signals were electronically measured
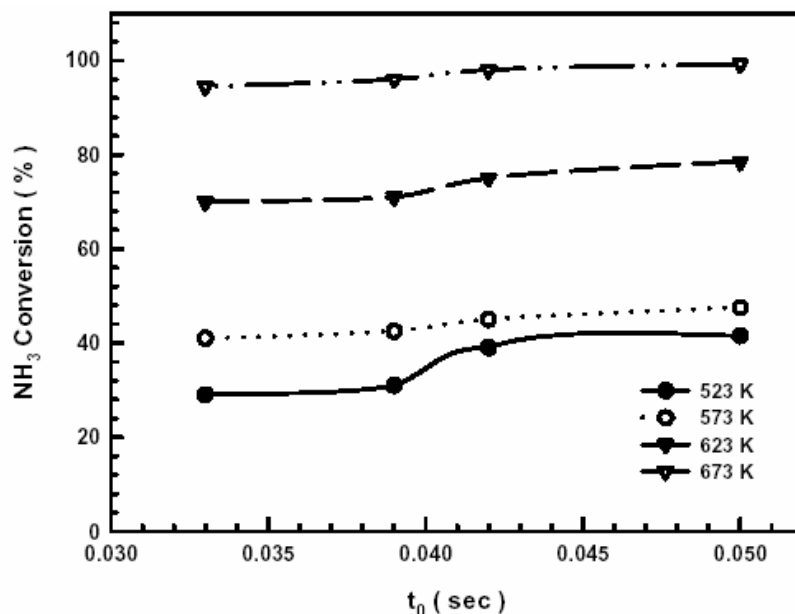
**Fig. 2.** Effect of empty bed residence time (EBRT) on the bimetallic $CuO/CeO_2$ nanoparticle catalyst for the conversion of $NH_3$ as function of temperature. Test conditions: 800 ppm $NH_3$ in He, $O_2 = 4\%$, GHSV = 92000 mL/h-g.

using a data integrator (CR-6A, Shimadzu, Kyoto, Japan). Dilute sulfuric acid was used to scrub the residual ammonia in the vapor gas and the amount present was measured using a Merck kit (Merck, Spectroquant Vega 400, Darmstadt, Germany). The concentrations of NO, $NO_2$ and $O_2$ in the gas samples were monitored continuously during combustion at a particular location, using a portable flue gas analyzer (IMR-3000, Neckarsulm, Germany). Data were collected when the SCO reaction was in a steady state, typically after 20 min at each temperature. Each temperature was maintained for 90 min to allow the system to enter a steady state. Most experiments were repeated once to ensure reproducibility, and similar results were always obtained.

## RESULTS AND DISCUSSION

Fig. 2 plots the effect on the reduction of $NH_3$ of the bimetallic $CuO/CeO_2$ nanoparticle catalyst used in the oxidation of $NH_3$ stream, in terms of the reaction temperature and the empty bed residence time (EBRT) of the influent stream. The results indicate that increasing the EBRT increased the efficiency of oxidation of $NH_3$. Increasing the reaction temperature was also observed to increase the extent of $NH_3$ oxidation. When the EBRT of the influent stream was set to 0.05 sec, about 98.0% of the $NH_3$ was reduced at 673K in the catalytic run, whereas only a 38.0% of $NH_3$ was removed using the catalysis at 523K. Normally, the amount of $NH_3$ removed by the catalyzed reaction was observed to be around 98.0% greater than that observed to be removed by the SCO process runs at 673K at a EBRT of under 0.05 sec.

With reference to the composition of copper

**Table 1.** Surface composition analysis of the test catalyst.

| Element percentage (%) | 6:4 [a] | 6:4 [b] |
|---|---|---|
| Cu [c] | 61.12 | 58.52 |
| Ce [c] | 38.82 | 35.01 |
| C [d] | 0.32 | 0.29 |
| H [d] | 0.35 | 0.33 |
| O [d] | 10.36 | 10.70 |
| N [d] | 0 | 0 |

[a] New catalyst.

[b] Used catalyst after 72 hours in fixed bed oxidation reactor.

[c] Determined by EDX.

[d] Determined by carbon-hydrogen-nitrogen elemental analysis.

and cerium from the catalyst, as presented in Table 1, analysis of the elemental composition of the surfaces of the test catalysts reveals that the composition of metal ions from the bimetallic $CuO/CeO_2$ nanoparticle catalyst varied slightly. The element oxygen percentage increasing in the catalyst surface, as shown in Table 1, is due to the oxygen ions conducted by $CeO_2$, in which the structure has a synergistic $Cu-O_{vacancy}$ interaction sites in nanoparticles (Sasi *et al.*, 2003). In greater detail, the oxygen that oxidizes ammonia over the bimetallic $CuO/CeO_2$ nanoparticle catalys is present in the lattice structure of the catalyst (as β oxygen) and as adsorbed oxygen (α oxygen). α oxygen is related to the oxygen vacancy of catalyst surface: α oxygen content increases with the number of oxygen vacancies (Sedmak *et al.*, 2003).

The adsorptive and catalytic behavior of a catalyst is strongly influenced by the capacity and texture of its exterior surface. Fig. 3. summarizes the properties of test catalysts determined by BET (Brunauer-Emmett-Teller method) analysis, including specific surface area. The specific surface area was 60 $m^2/g$ at 523K. At the 673K on a bimetallic $CuO/CeO_2$ nanoparticle catalyst, the surface areas slightly decreased (43 $m^2/g$). This test showed that the catalysts were associated with a larger lattice surface of copper or cerium, and that higher temperature caused metal sintering, perhaps reducing catalytic activity. Clearly, reaction temperature conditions are important role in activating the generated surface, and the increase in surface area may not be the main factor in that promotes the activity.

The overall selectivity of $N_2$ production varied from 19-85% and that of NO production varied from 0-4% over the range of 11.0-98.0% $NH_3$ conversion at $NH_3$ concentrations of 800 ppm (Fig. 4). Nitrogen gas thought to be formed primarily by the dissociation of NO produced by oxidation of adsorbed $NH_3$ (Bradley *et al.*, 1995). Therefore, we hypothesis that $NH_3$ and oxygen may be adsorbed onto specific sites on the bimetallic $CuO/CeO_2$ nanoparticle catalyst, promoting the rapid conversion of $NH_3$ to nitrogen and water. Nitrogen was the
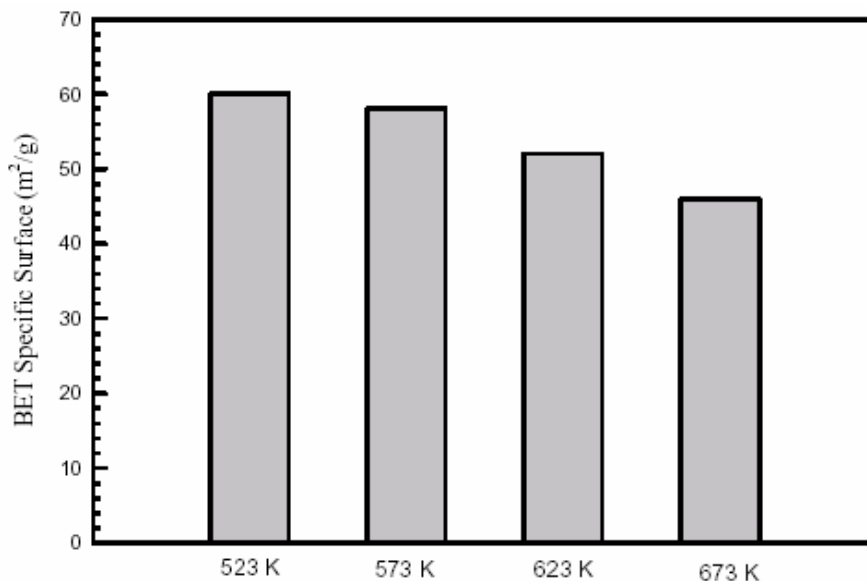
**Fig. 3.** Effect of reaction temperature with changes of specific surface area on the bimetallic $CuO/CeO_2$ nanoparticle catalyst for the conversion of $NH_3$. Test conditions: 800 ppm $NH_3$ in He, $O_2$ = 4%, RH = 18%, GHSV = 92000 mL/h-g.
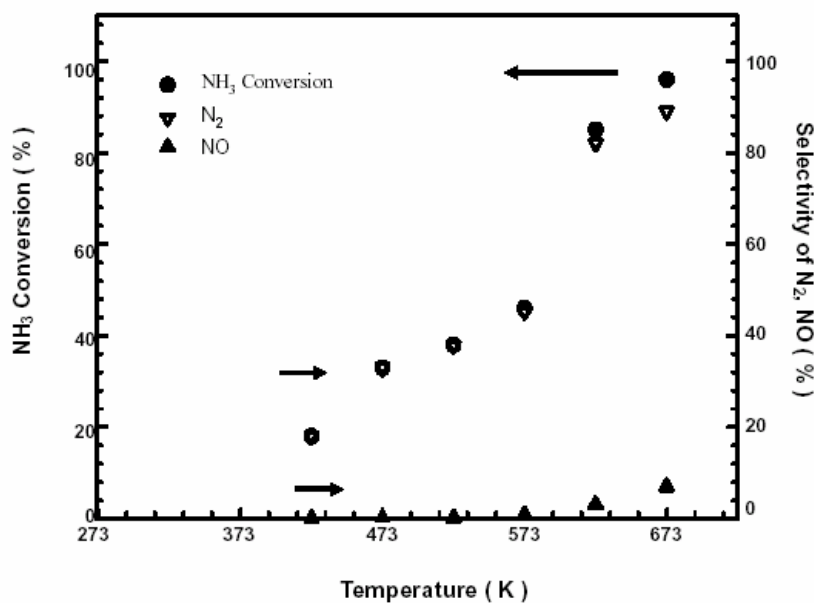


**Fig. 4.** Relationship of the ammonia conversion, $N_2$ yield, and NO yield at various temperatures over the bimetallic $CuO/CeO_2$ nanoparticle catalyst. Test conditions: 800 ppm $NH_3$ in He, $O_2$ = 4%, RH = 12%, Temp = 423-673K, GHSV = 92000 mL/h-g.

dominant gaseous, and a small amount of NO was detected in the resultant stream. This result is similar to that obtained by Curtin *et al.* (2000).
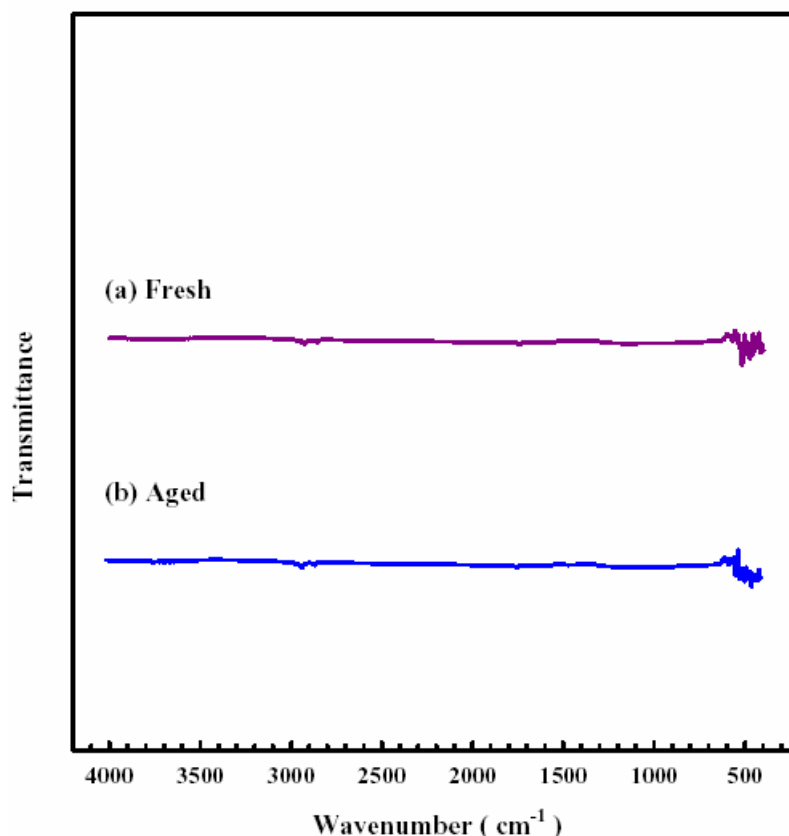
**Fig. 5.** ATR-FTIR pattern of the bimetallic $CuO/CeO_2$ nanoparticle catalyst. (a) fresh, (b) after activity test. Test conditions: 800 ppm $NH_3$ in He, $O_2 = 4\%$, GHSV = 92000 mL/h-g.

Fig. 5. compares the ATR-FTIR spectra of fresh and used catalysts, also verifying the presence of the CuO-like phase 510 $cm^{-1}$ of the catalyst (Sadykov *et al.*, 2001). As illustrated in Fig. 5, the monodentate nitrite, nitro group anions and hydroxyl groups on the framework are associated with a peak at about 2990 $cm^{-1}$ and 2820 $cm^{-1}$ for used catalysts (Blanco *et al.*, 1993).

The change in the sizes of particles of the catalyst was determined using the laser light-scattering method, as depicted in Fig. 6. The mean particle size converged to approximately 15.9 μm for fresh bimetallic

$CuO/CeO_2$ nanoparticle catalyst. However, the diameters of the catalyst declined after activity test and the mean particle size was around 13.3 μm, indicating that co-precipitation aggregates the high reaction temperature. Hence, such changes in the sizes of particles of the catalyst can be attributed to over-oxidation of the bimetallic $CuO/CeO_2$ nanoparticle catalyst surface during the reaction.

Fig. 7. presents the surface morphological changes of bimetallic $CuO/CeO_2$ nanoparticle catalyst elucidating using TEM to provide information on the fresh/aged catalyst surface
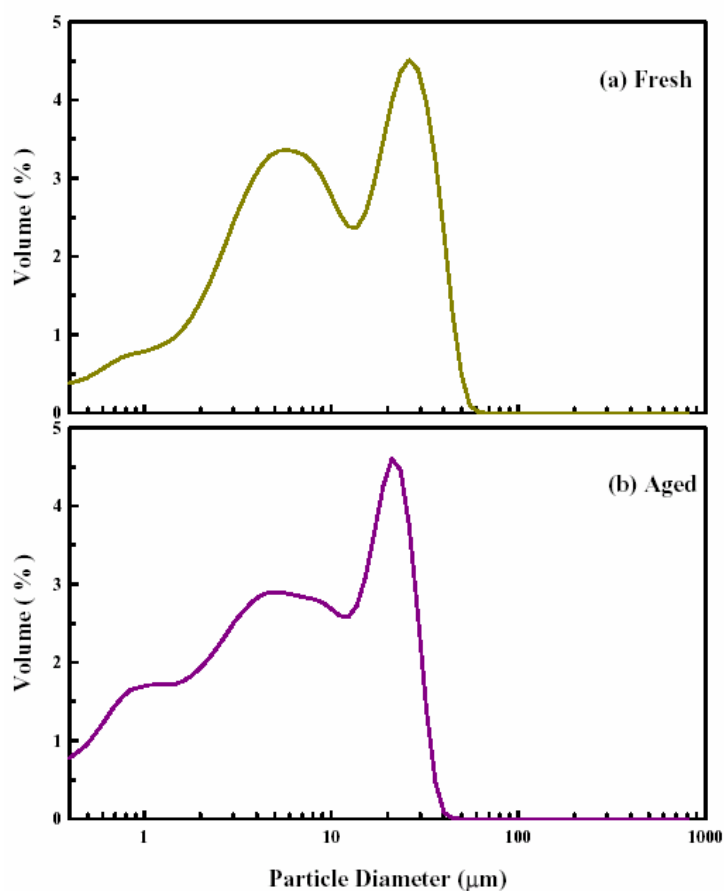
**Fig. 6.** Changes in particle sizes distribution of the bimetallic CuO/CeO$_2$ nanoparticle catalyst. (a) fresh, (b) after activity test. Test conditions: 800 ppm NH$_3$ in He, O$_2$ = 4%, GHSV = 92000 mL/h-g.
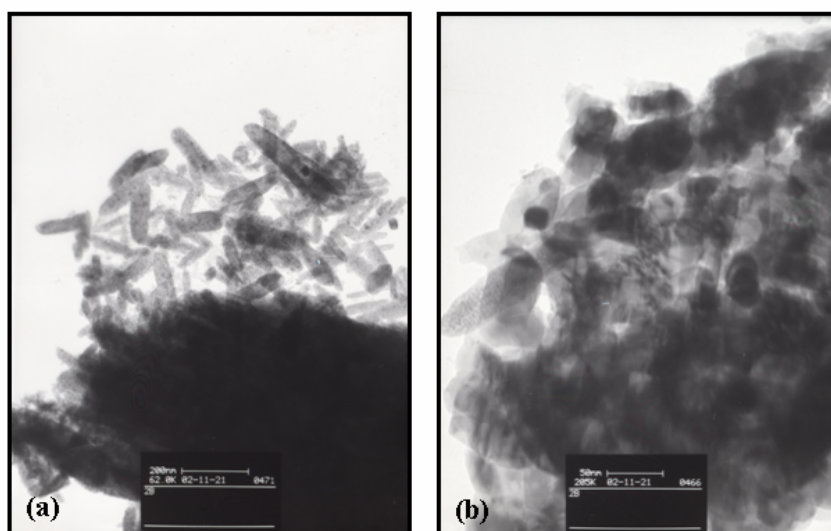


**Fig. 7.** TEM photograph of (a) fresh and (b) after activity test bimetallic CuO/CeO$_2$ nanoparticle catalyst. Test conditions: 800 ppm NH$_3$ in He, O$_2$ = 4%, GHSV = 92000 mL/h-g.

structure. Fig. 7a. indicates that bimetallic $CuO/CeO_2$ nanoparticle catalyst exhibits more aggregation and crystalline than observed in Fig. 7b. These crystallinity phases may explain the high activity of the catalysts. Fig. 7b. indicates that disaggregated phases were formed when the surface of the catalyst was aged or when poisoning occurred because of plugging, implying that the porosity of the particles had changed. Based on the above results, it also can be confirmed that the dispersion phenomena of the bimetallic $CuO/CeO_2$ nanoparticle catalyst increase the efficiency of removal of $NH_3$.

## CONCLUSIONS

The present study has shown that selective catalytic oxidation for ammonia ($NH_3$-SCO) by a bimetallic $CuO/CeO_2$ nanoparticle catalyst was found to promote the oxidation of $NH_3$. The SCO process was found to be more effective at lower temperatures. The process altered the oxidation state and the crystalline composition of the catalyst. The overall by-product selectivity of the production of NO varied from 0-4% and that of $N_2$ production varied from 19-85% at 20.0-98.0% $NH_3$ conversion, when a bimetallic $CuO/CeO_2$ nanoparticle catalyst was used. Also, changes in oxidation state and the crystalline composition of the catalyst were identified. This work shows that the SCO process has the potential to treat highly concentrated streams of $NH_3$, helping industrial plants to meet discharge regulations.

## ACKNOWLEDGMENTS

## REFERENCES

Blanco, J., Avila, P. and Fierro, J.L.G. (1993). Influence of Nitrogen Dioxide on the Selective Reduction of NOx with a Catalyst of Copper and Nickel Oxides. *Appl. Catal. A* 96: 331-343.

Bradely, J.M., Hopkinson, A. and King, D.A. (1995). Control of a Biphasic Surface Reaction by Oxygen Coverage: the Catalytic Oxidation of Ammonia over Pt {100}. *J. Phys. Chem.* 99: 17032-17042.

Chou, M.S. and Wang, C.H. (2007). Treatment of Ammonia in Air Stream by Biotrickling Filter. *Aerosol Air Qual. Res.* 7: 17-32.

Curtin, T., Regan, F.O., Deconinck, C., Knűttle, N. and Hodnett, B.K. (2000). The Catalytic Oxidation of Ammonia: Influence of Water and Sulfur on Selectivity to Nitrogen over Promoted Copper Oxide/Alumina Catalysts. *Catal. Today* 55: 189-195.

Dravell, L.I., Heiskanen, K., Jones, J.M., Ross, A.B., Simell, P. and Williams, A. (2003). An Investigation of Alumina-Supported Catalysts for the Selective Catalytic Oxidation of Ammonia in Biomass Gasification. *Catal. Today* 81: 681-692.

Geng, Q., Guo, Q., Cao, C., Zhang, Y. and

Wang, L. (2008). Investigation into Photocatalytic Degradation of Gaseous Ammonia in CPCR. *Ind. Eng. Chem. Res.* 47, 4363-4368.

Hung, C.M. (2006). Selective Catalytic Oxidation of Ammonia to Nitrogen on CuO-CeO$_2$ Bimetallic Oxide Catalysts. *Aerosol Air Qual. Res.* 6: 150-169.

Hung, C.M. (2008). Decomposition Kinetics of Ammonia in Gaseous Stream by a Nanoscale Copper-Cerium Bimetallic Catalyst. *J. Haz. Mat.* 150: 53-61.

Il'chenko, N.I. (1976). Catalytic Oxidation of Ammonia. *Russ. Chem. Rev.* 45: 1119-1134.

Kundakovic, L. and Flytzani-Stephanopoulos, M. (1998). Reduction Characteristics of Copper Oxide in Cerium and Zirconium Oxide Systems. *Appl. Catal. A: Gen.* 171: 13-29.

Liang, C., Li, W., Wei, Z., Xin, Q. and Li, C. (2000). Catalytic Decomposition of Ammonia over Nitrided MoNx/α-Al$_2$O$_3$ and NiMoNy/α-Al$_2$O$_3$ Catalysts. *Ind. Eng. Chem. Res.* 39: 3694-3697.

Lin, C.H., Wu, Y.L., Lai, C.H., Watson, J.G. and Chow, J.C. (2008). Air Quality Measurements from the Southern Particulate Matter Supersite in Taiwan. *Aerosol Air Qual. Res.* 8: 233-264.

Ng, P.F., Li, L., Wang, S., Zhu, Z., Lu, G. and Yan, Z. (2007). Catalytic Ammonia Decomposition over Industrial-Waste-Supported Ru Catalysts. *Environ. Sci. Technol.* 41: 3758-3762.

Pansare, S.S. and Jr. Goodwin, J.G. (2008). Ammonia Decomposition on Tungsten-Based Catalysts in the Absence and Presence of Syngas. *Ind. Eng. Chem. Res.* 47: 4063-4070.

Sadykov, V.A., Bunina, R.V., Alikina, G.M., Ivanova, A.S., Kochubei, D.I., Novgorodov, B.N., Paukshtis, E.A., Fenelonov, V.B., Zaikovskii, V.I. and Kuznetsova, T.G. (2001). Supported CuO + Ag/partially Stabilized Zirconia Catalysts for the Selective Catalytic Reduction of NO$_x$ under Lean Burn Conditions : 1. Bulk and Surface Properties of the Catalysts. *J. Catal.* 200: 117-130.

Sasi, F., Duprez, D., Gérard, F. and Miloudi, A. (2003). Hydrogen Formation in the Reaction of Steam with Rh/CeO$_2$ Catalyst: a Tool for Characterizing Reduced Centers of Ceria. *J. Catal.* 213: 226-234.

Schmidt-Szałowski, K., Krawczyk, K. and Petryk, J. (1998). The Properties of Cobalt Oxide Catalyst for Ammonia Oxidation. *Appl. Catal. A: Gen.* 175: 147-157.

Sedmak, G., Hočevar, S. and Levec, J. (2003). Kinetics of Selective CO Oxidation in Excess of H$_2$ over the Nanostructured Cu$_{0.1}$Ce$_{0.9}$O$_{2-y}$ Catalyst. *J. Catal.* 213: 135-150.

Skårman, B., Grandjean, D., Benfield, R.E., Hinz, A., Andersson, A. and Wallenberg, L.R. (2002). Carbon Monoxide Oxidation on Nanostructured CuO$_x$/CeO$_2$ Composite Particles Characterized by HREM, XPS, XAS, and High-Energy Diffraction. *J. Catal.* 211: 119-133.

Wang, W., Padban, N., Ye, Z., Andersson, A. and Bjerle, I. (1999). Kinetic of Ammonia Decomposition in Hot Gas Cleaning. *Ind.*

*Eng. Chem. Res.* 38: 4175-418.

Xu, X., Barsha, N. and Li, J. (2008).
Analyzing Regional Influence of Particulate
Matter on the City of Beijing, China.

*Aerosol Air Qual. Res.* 8: 78-93.